FLOW AND HEAT TRANSFER OF THREE IMMISCIBLE FLUIDS IN THE PRESENCE OF ELECTRIC AND INCLINED MAGNETIC FIELD

by

Živojin M. STAMENKOVIĆ[a*], Miloš M. KOCIĆ[a], Jelena D. PETROVIĆ[a] and Milica D. NIKODIJEVIĆ[b]

[a] Faculty of Mechanical Engineering, University of Nis, Nis, Serbia
[b] Faculty of Occupational Safety, University of Nis, Nis, Serbia

Original scientific paper
https://doi.org/10.2298/TSCI18S5575S

The MHD flow of three immiscible fluids in a horizontal channel with isothermal walls in the presence of an applied electric and inclined magnetic field has been investigated in the paper. All three fluids are electrically conducting, while the channel plates are electrically insulated. The general equations that describe the discussed problem under the adopted assumptions are reduced to ODE and closed-form solutions are obtained in three fluid regions of the channel. Separate solutions with appropriate boundary and interface conditions for each fluid have been determined. The analytical results for various values of the Hartmann number, magnetic field inclination angle, ratio of fluid viscosities, and electrical conductivities have been presented graphically to show their effect on the flow and heat transfer characteristics.

Key words: *immiscible fluids, heat transfer, Hartmann number, loading parameter, magnetic field*

Introduction

The flow of electrically conducting viscous fluids between two parallel plates in the presence of a transversely applied magnetic field has applications in many technical processes and devices. The interest in effects of outer magnetic field on heat-physical processes appeared in the early seventies of the last century. Blum [1] presented one of the first works in the field of mass and heat transfer in the presence of magnetic field. Many researchers [2, 3] have studied the MHD flow and heat transfer of Newtonian and non-Newtonian conducting fluids. One of them is also Attia [4] who investigated the Hall current effects on the velocity and temperature fields of an unsteady Hartmann flow. Recently, Kiyasatfar *et al.* [5] presented investigation of thermal behavior and fluid motion in DC MHD pumps, Chandrasekhar and Sharma [6] presented heat transfer of a nanofluid in a circular duct, while Abou-Zeid [7] gives the solution for MHD non-Newtonian nanofluid flow through a porous medium in eccentric annuli.

The problem of convective MHD channel flow between two parallel plates subjected simultaneously to an axial temperature gradient and pressure gradient was studied numerically by Ghosh and Nandi [8]. One decade ago, Bodosa and Borkakati [9] analyzed the prob-

* Corresponding author, e-mail: zivojin.stamenkovic@masfak.ni.ac.rs

lem of an unsteady 2-D flow of viscous incompressible and electrically conducting fluid between two parallel plates in the presence of a uniform transverse magnetic field, for the case of isothermal plates and one isothermal and other adiabatic. Ghosh *et al.* [10] has obtained an analytical solution to the problem of hydromagnetic free convection flow with induced magnetic field effects. Of course there are many other investigations, like Borkakati and Chakrabarty [11] investigation of unsteady free convection MHD flow between two heated vertical parallel plates in induced magnetic field, or Aydin and Avci [12] analytical investigation of laminar heat convection in a Couette-Poiseuille flow between two parallel plates with a simultaneous pressure gradient and an axial movement of the upper plate. Recently, an analytical solution is suggested by Singa [13] for the problem of MHD free convective flow of an electrically conducting fluid between two heated parallel plates in the presence of an induced magnetic field.

All the mentioned studies refer to a single-fluid model. Most of the problems relating to the petroleum industry, geophysics, plasma physics, MHD, and so forth involve multi-fluid flow situations. Because of that, Shail [14] studied Hartmann flow of conducting fluid and a non-conducting fluid layer contained in channel and his results predicted that an increase of the order of 30% can be achieved in the flow rate suitable ratios of heights and viscosities of the two fluids. Lohrasbi and Sahai [15] studied two-phase MHD flow and heat transfer in parallel plate channel with the fluid in one-phase being conducting. There have been some experimental and analytical studies on hydrodynamic aspects of the two fluid-flow reported in the recent literature. Malashetty [16] have studied the two fluid MHD flow and heat transfer in an inclined channel containing porous and fluid layer, while Abou-Zeid [17] analyzed MHD internal heat generation in a porous medium. Recently, Umavathi [18] have analyzed the MHD Poiseuille-Couette flow and heat transfer of two immiscible fluids between inclined parallel plates.

Due the importance of the two fluid-flow models, in our previous paper [19] flow and heat transfer of two immiscible fluids in the presence of uniform inclined magnetic field was investigated. While most of the previous studies mainly consider two fluid-flow, there is a model which discuss the combined effects of pressure gradient and electroosmosis for the three fluid-flow [20]. Multi-layer flows occur industrially in three main settings. Firstly there are co-extrusion processes, where a product is made of more than one layer simultaneously. Secondly, there are film-coating processes, where a layer is applied to a fluid substrate. Thirdly, there are lubricated transport processes, where a lubricating fluid lies in a layer between the wall of a duct and the transported fluid [21]. The development of microfluidics platforms in recent years has led to an increase in the number of applications involving the flow of multiple immiscible layers of viscous electrolyte fluids [22]. Recent studies show that MHD flows can also be a viable option for transporting weekly conducting fluids in microscale systems, such as flow inside the micro-channel networks of a lab-on-a-chip device [23, 24]. In micro-fludic devices, multiple fluids may be transported through a channel for various reasons. For example, increase an mobility of a fluid can be achieved by stratification of highly mobile fluid or mixing of two or more fluids in transit may be designed for heat and mass transfer applications. In that regard, magnetic field-driven micropumps are in increasing demand due to their reliability, absence of moving parts, low power, flow reversibility and mixing efficiency [25, 26].

Three fluid-flow is widely encountered in the petroleum industry, Thorn *et al.*, [27]. A good understanding of three fluid-flow is of practical importance, *e. g.* flow of water, oil and gas in the oil transportation pipelines. In these systems, the three fluids are generally separated by interfaces. These interfaces determine the flow pattern that is closely related to the pressure drop and gas holdup in the pipes. For the safety operation of the systems, the distribution of the three fluids in the pipes is very important. There are different approaches to model the interfaces of fluids and in this paper, a planar interface between the three immiscible fluids is assumed.

Mathematical model

As already mentioned, the MHD flow of three immiscible fluids in a horizontal channel with isothermal walls in the presence of an applied electric and inclined magnetic field has been investigated in the paper.

The fluids in the three regions have been assumed immiscible and incompressible and the flow has been steady, 1-D and fully developed. All three fluids have different kinematic viscosities ν_1, ν_2, and ν_3 and densities ρ_1, ρ_2, and ρ_3. The analytical solutions for velocities, magnetic field, and temperature distribution have been obtained and computed for different values of the characteristic parameters. The physical model, shown in fig. 1, consists of two infinite parallel plates extending in the x- and z-direction. In the region I $h \le y \le 2h$ we have fluid of dynamic viscosity μ_1, electrical conductivity σ_1, thermal conductivity, k_1, and specific heat capacity, c_{p1}, then goes the region II $0 \le y \le h$ which has been filled by a layer of different fluid of dynamic viscosity μ_2, electrical conductivity σ_2, thermal conductivity k_2, and specific heat capacity c_{p2} and the last region III $-h \le y \le 0$ has been filled by a layer of fluid of dynamic viscosity, μ_3, electrical conductivity, σ_3, thermal conductivity, k_3, and specific heat capacity, c_{p3}.

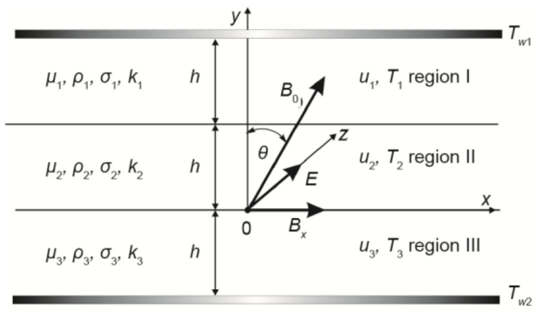

Figure 1. Physical model and co-ordinate system

A uniform magnetic field of the strength $\vec{\mathrm{B}}$ and $\vec{\mathrm{v}}$ we are considering 1-D flow in x-direction:

$$\vec{\mathrm{v}} = u\vec{i} \tag{1}$$

$$\vec{\mathrm{B}} = \left[B_x(y) + B_0\sqrt{1-\lambda^2}, B_0\lambda, 0 \right] \tag{2}$$

where $\vec{\mathrm{B}}$ is the magnetic field vector, $\vec{\mathrm{v}}$ – the flow velocity vector, and $\lambda = \cos\theta$. The upper and lower plates have been kept at the two constant temperatures T_{w1} and T_{w2}, respectively, and the plates are electrically insulated. We are considering a stationary problem $(\partial/\partial t = 0)$. The described MHD three fluid flow problem is mathematically presented with equations:

$$\frac{1}{\rho_i}P + \nu\frac{\partial^2 u_i}{\partial y^2} - \frac{\sigma_i B_0\lambda(E_z + u_i B_0\lambda)}{\rho_i} = 0 \tag{3}$$

$$B_0\lambda\frac{\mathrm{d}u_i}{\mathrm{d}y} + \frac{1}{\sigma_i\mu_{ei}}\frac{\partial^2 B_{xi}}{\partial y^2} = 0 \tag{4}$$

$$k_i \frac{\mathrm{d}^2 T_i}{\mathrm{d}y^2} + \mu_i \left(\frac{\mathrm{d}u_i}{\mathrm{d}y}\right)^2 + \sigma_i (E_z + u_i B_0 \lambda)^2 = 0 \tag{5}$$

where

$$P = -\frac{\partial p}{\partial x} \tag{6}$$

The fluid and thermal boundary conditions for this problem are represented by:

$$u_1(2h) = 0, \qquad u_1(h) = u_2(h), \qquad u_2(0) = u_3(0), \qquad u_3(-h) = 0 \tag{7}$$

$$\mu_1 \frac{\mathrm{d}u_1}{\mathrm{d}y}\bigg|_{y=h} = \mu_2 \frac{\mathrm{d}u_2}{\mathrm{d}y}\bigg|_{y=h}, \qquad \mu_2 \frac{\mathrm{d}u_2}{\mathrm{d}y}\bigg|_{y=0} = \mu_3 \frac{\mathrm{d}u_3}{\mathrm{d}y}\bigg|_{y=0} \tag{8}$$

$$B_{x1}(2h) = 0, \qquad B_{x1}(h) = B_{x2}(h), \qquad B_{x2}(0) = B_{x3}(0), \qquad B_{x3}(-h) = 0 \tag{9}$$

$$\frac{1}{\sigma_1 \mu_{e1}} \frac{\mathrm{d}B_{x1}}{\mathrm{d}y}\bigg|_{y=h} = \frac{1}{\sigma_2 \mu_{e2}} \frac{\mathrm{d}B_{x2}}{\mathrm{d}y}\bigg|_{y=h}, \qquad \frac{1}{\sigma_2 \mu_{e2}} \frac{\mathrm{d}B_{x2}}{\mathrm{d}y}\bigg|_{y=0} = \frac{1}{\sigma_3 \mu_{e3}} \frac{\mathrm{d}B_{x3}}{\mathrm{d}y}\bigg|_{y=0} \tag{10}$$

$$T_1(2h) = T_{w1}, \qquad T_1(h) = T_2(h), \qquad T_2(0) = T_3(0), \qquad T_3(-h) = T_{w2} \tag{11}$$

$$k_1 \frac{\mathrm{d}T_1}{\mathrm{d}y}\bigg|_{y=h} = k_2 \frac{\mathrm{d}T_2}{\mathrm{d}y}\bigg|_{y=h}, \qquad k_2 \frac{\mathrm{d}T_2}{\mathrm{d}y}\bigg|_{y=0} = k_3 \frac{\mathrm{d}T_3}{\mathrm{d}y}\bigg|_{y=0}. \tag{12}$$

Now, the following transformations have been used to transform previous equations to dimensionless form:

$$u_i^* = \frac{u_i}{U_0}, \qquad y^* = \frac{y}{h}, \qquad \alpha_1 = \frac{\mu_1}{\mu_2}, \qquad \alpha_2 = \frac{\mu_2}{\mu_3}, \qquad \gamma_1 = \frac{\sigma_1}{\sigma_2}$$

$$\gamma_2 = \frac{\sigma_2}{\sigma_3}, \qquad \xi_1 = \frac{k_2}{k_1}, \qquad \xi_2 = \frac{k_3}{k_2}, \qquad \delta_1 = \frac{\mu_{e1}}{\mu_{e2}}, \qquad \delta_2 = \frac{\mu_{e2}}{\mu_{e3}} \tag{13}$$

$$G_i = \frac{P}{\frac{\mu_i U_0}{h^2}}, \qquad b_i = \frac{B_{xi}}{B_0} \tag{14}$$

– Load factor

$$K = \frac{E_z}{U_0 B_0} \tag{15}$$

– Hartmann number

$$\mathrm{Ha}_i = B_0 h \sqrt{\frac{\sigma_i}{\mu_i}} \tag{16}$$

– Magnetic Reynolds number

$$\mathrm{R}_{\mathrm{m}i} = U_0 h \sigma_i \mu_{ei} \tag{17}$$

– Prandtl number

$$\mathrm{Pr}_i = \frac{\mu_i c_{pi}}{k_i} \tag{18}$$

– Eckert number

$$\mathrm{Ec}_i = \frac{U_{\mathrm{ref}}}{c_{pi}(T_{w1} - T_{w2})} \tag{19}$$

Using the transformations we obtain eqs. (3)-(5) in the next form:

$$\frac{\mathrm{d}^2 u_i^*}{\mathrm{d}y^{*2}} - \lambda\,\mathrm{Ha}_i^{\,2}(K + u_i^*\lambda) + G_i = 0 \tag{20}$$

$$\frac{\mathrm{d}^2 b_i}{\mathrm{d}y^{*2}} + \lambda R_{m_i}\frac{\mathrm{d}u_i^*}{\mathrm{d}y^*} = 0 \tag{21}$$

$$\frac{\mathrm{d}^2\theta_i}{\mathrm{d}y^{*2}} + \mathrm{Pr}_i\,\mathrm{Ec}_i\left(\frac{\mathrm{d}u_i^*}{\mathrm{d}y^*}\right)^2 + \mathrm{Pr}_i\,\mathrm{Ec}_i\,\mathrm{Ha}_i^2(K + \lambda u_i^*)^2 = 0 \tag{22}$$

The boundary dimensionless conditions for previous equations are:

$$u_1^*(2) = 0, \qquad u_1^*(1) = u_2^*(1), \qquad u_2^*(0) = u_3^*(0), \qquad u_3^*(-1) = 0 \tag{23}$$

$$\alpha_1\frac{\mathrm{d}u_1^*}{\mathrm{d}y^*} = \frac{\mathrm{d}u_2^*}{\mathrm{d}y^*}, \qquad y^* = 1, \qquad \alpha_2\frac{\mathrm{d}u_2^*}{\mathrm{d}y^*} = \frac{\mathrm{d}u_3^*}{\mathrm{d}y^*}, \qquad y^* = 0\,, \tag{24}$$

$$b_1(2) = 0, \qquad b_1(1) = b_2(1), \qquad b_2(0) = b_3(0), \qquad b_3(-1) = 0 \tag{25}$$

$$\frac{\mathrm{d}b_1}{\mathrm{d}y^*} = \gamma_1\delta_1\frac{\mathrm{d}b_2}{\mathrm{d}y^*}, \qquad y^* = 1, \qquad \frac{\mathrm{d}b_2}{\mathrm{d}y^*} = \gamma_2\delta_2\frac{\mathrm{d}b_3}{\mathrm{d}y^*}, \qquad y^* = 0 \tag{26}$$

The solution of transformed eqs. (20)-(22), with boundary conditions, has the following form:

$$u_i^*(y^*) = A_i\cosh(\lambda\,\mathrm{Ha}_i\,y^*) + C_i\sinh(\lambda\,\mathrm{Ha}_i\,y^*) + F_i \tag{27}$$

$$b_i(y^*) = -\frac{R_{mi}}{\mathrm{Ha}_i}[A_i\sinh(\lambda\,\mathrm{Ha}_i\,y^*) - C_i\cosh(\lambda\,\mathrm{Ha}_i\,y^*)] + Q_i y^* + R_i \tag{28}$$

$$\theta_i(y^*) = -\frac{\mathrm{Ec}_i\,\mathrm{Pr}_i}{4\lambda}[\lambda(A_i^2 + C_i^2)\cosh(2\lambda\,\mathrm{Ha}_i\,y^*) + 2A_iC_i\lambda\sinh(2\lambda\,\mathrm{Ha}_i\,y^*) +$$

$$+ 8A_iS_i\cosh(\lambda\,\mathrm{Ha}_i\,y^*) + 8C_iS_i\sinh(\lambda\,\mathrm{Ha}_i\,y^*) + 2\lambda\,\mathrm{Ha}_i^{\,2}\,S_i^{\,2}y^{*2}] + L_i y^* + M_i \tag{29}$$

where

$$F_i = \frac{G_i}{\lambda^2\,\mathrm{Ha}_i^{\,2}} - \frac{K}{\lambda} \tag{30}$$

and constants for velocity filed are:

$$C_1 = -\frac{F_1 + A_1 \cosh(2\lambda \,\mathrm{Ha}_1)}{\sinh(2\lambda \,\mathrm{Ha}_1)}, \quad C_2 = -A_1 D_1 + F_1 D_2 + F_2 \sinh(\lambda \,\mathrm{Ha}_2), \quad C_3 = \frac{\alpha_2 C_2 \,\mathrm{Ha}_2}{\mathrm{Ha}_3} \tag{31}$$

$$A_1 = \frac{[F_1 D_2 + F_2 \sinh(\lambda \,\mathrm{Ha}_2)] D_3}{\mathrm{Ha}_3 \cosh(\lambda \,\mathrm{Ha}_3) \sinh(\lambda \,\mathrm{Ha}_1) + D_1 D_3} + \frac{-F_1 D_4 + F_2 D_5 - F_3 D_6}{\mathrm{Ha}_3 \cosh(\lambda \,\mathrm{Ha}_3) \sinh(\lambda \,\mathrm{Ha}_1) + D_1 D_3}$$

$$A_2 = \frac{A_1 \cosh(\lambda \,\mathrm{Ha}_1) + C_1 \sinh(\lambda \,\mathrm{Ha}_1)}{\cosh(\lambda \,\mathrm{Ha}_2)} + \frac{-C_2 \sinh(\lambda \,\mathrm{Ha}_2) + F_1 - F_2}{\cosh(\lambda \,\mathrm{Ha}_2)}$$

$$A_3 = A_2 + F_2 - F_3 \tag{32}$$

In previous constants following marks are used for the sake of shorter statement:

$$D_1 = \frac{\sinh(\lambda \,\mathrm{Ha}_2)}{2\cosh(\lambda \,\mathrm{Ha}_1)} + \frac{\alpha_1 \,\mathrm{Ha}_1 \cosh(\lambda \,\mathrm{Ha}_2)}{2\,\mathrm{Ha}_2 \sinh(\lambda \,\mathrm{Ha}_1)} \tag{33}$$

$$D_2 = \frac{\sinh(\lambda \,\mathrm{Ha}_2)}{2\cosh(\lambda \,\mathrm{Ha}_1)} - \frac{\alpha_1 \,\mathrm{Ha}_1 \cosh(\lambda \,\mathrm{Ha}_2)}{2\,\mathrm{Ha}_2 \sinh(\lambda \,\mathrm{Ha}_1)} - \sinh(\lambda \,\mathrm{Ha}_2) \tag{34}$$

$$D_3 = \sinh(2\lambda \,\mathrm{Ha}_1) \,\mathrm{Ha}_3 \sinh(\lambda \,\mathrm{Ha}_2) \cosh(\lambda \,\mathrm{Ha}_3) +$$

$$+ \alpha_2 \,\mathrm{Ha}_2 \sinh(2\lambda \,\mathrm{Ha}_1) \cosh(\lambda \,\mathrm{Ha}_2) \sinh(\lambda \,\mathrm{Ha}_3) \tag{35}$$

$$D_4 = \mathrm{Ha}_3 \cosh(\lambda \,\mathrm{Ha}_3) [\sinh(2\lambda \,\mathrm{Ha}_1) - \sinh(\lambda \,\mathrm{Ha}_1)] \tag{36}$$

$$D_5 = \mathrm{Ha}_3 \cosh(\lambda \,\mathrm{Ha}_3) \sinh(2\lambda \,\mathrm{Ha}_1) [1 - \cosh(\lambda \,\mathrm{Ha}_2)] \tag{37}$$

$$D_6 = \mathrm{Ha}_3 \cosh(\lambda \,\mathrm{Ha}_2) \sinh(2\lambda \,\mathrm{Ha}_1) [1 - \cosh(\lambda \,\mathrm{Ha}_3)] \tag{38}$$

Then the constants for magnetic field are:

$$Q_1 = \Im_2 - \Im_3 - R_1 + Q_2 + R_2 \tag{39}$$

$$Q_2 = \frac{\Im_1 - \Im_2 + \Im_3 - \Im_5 + \Im_6 - \Im_4 - Q_3}{1 + \delta_1 \gamma_1} \tag{40}$$

$$Q_3 = \frac{\Im_1 - \Im_2 + \Im_3 - \Im_4 - \Im_5 + \Im_6}{1 + \delta_2 \gamma_2 (1 + \delta_1 \gamma_1)} - \frac{(1 + \delta_1 \gamma_1)(\lambda R_{m2} A_2 - \lambda \delta_2 \gamma_2 R_{m3} A_3)}{1 + \delta_2 \gamma_2 (1 + \delta_1 \gamma_1)} \tag{41}$$

$$R_1 = 2(\Im_2 - \Im_3) - \Im_1 + 2Q_2 + 2R_2 \tag{42}$$

$$R_2 = Q_3 + \Im_4 + \frac{R_{m2}}{\mathrm{Ha}_2} C_2 - \frac{R_{m3}}{\mathrm{Ha}_3} C_3 \tag{43}$$

$$R_3 = \Im_4 + Q_3 \tag{44}$$

where introduced marks are:

$$\Im_1 = \frac{R_{m1}}{\text{Ha}_1}[A_1 \sinh(2\lambda\,\text{Ha}_1) + C_1 \cosh(2\lambda\,\text{Ha}_1)] \tag{45}$$

$$\Im_2 = \frac{R_{m1}}{\text{Ha}_1}[A_1 \sinh(\lambda\,\text{Ha}_1) + C_1 \cosh(\lambda\,\text{Ha}_1)] \tag{46}$$

$$\Im_3 = \frac{R_{m2}}{\text{Ha}_2}[A_2 \sinh(\lambda\,\text{Ha}_2) + C_2 \cosh(\lambda\,\text{Ha}_2)] \tag{47}$$

$$\Im_4 = \frac{R_{m3}}{\text{Ha}_3}[-A_3 \sinh(\lambda\,\text{Ha}_3) + C_3 \cosh(\lambda\,\text{Ha}_3)] \tag{48}$$

$$\Im_5 = \lambda R_{m1}[A_1 \cosh(\lambda\,\text{Ha}_1) + C_1 \sinh(\lambda\,\text{Ha}_1)] \tag{49}$$

$$\Im_6 = \lambda R_{m2}\delta_1\gamma_1[A_2 \cosh(\lambda\,\text{Ha}_2) + C_2 \sinh(\lambda\,\text{Ha}_2)] \tag{50}$$

At the end constants for temperature are:

$$M_1 = 1 - N_1 - 2D_1, \qquad M_2 = -D_1 - D_2 - N_1 + N_2 - N_3 + 1 \tag{51}$$

$$M_3 = -D_1 - D_2 - N_1 + N_2 - N_3 + N_4 - N_5 + 1 \tag{52}$$

$$L_1 = \frac{(N_8 - N_7)(1+\xi_2) + \xi_1(N_{10} - N_9)}{(1+\xi_2+\xi_1\xi_2)} - \frac{\xi_1\xi_2(N_1 - N_2 + N_3 - N_4 + N_5 - N_6 - 1)}{(1+\xi_2+\xi_1\xi_2)} \tag{53}$$

$$L_2 = \frac{N_{10} - N_9 - \xi_2(L_1 + N_1 - N_2)}{1+\xi_2} - \frac{\xi_2(N_3 - N_4 + N_5 - N_6 - 1)}{1+\xi_2} \tag{54}$$

$$L_3 = -L_1 - L_2 - N_1 + N_2 - N_3 + N_4 - N_5 + N_6 + 1 \tag{55}$$

where introduced marks are:

$$N_1 = -\frac{\text{Ec}_1\,\text{Pr}_1}{4\lambda}[\lambda(A_1^2 + C_1^2)\cosh(4\lambda\,\text{Ha}_1) + 2A_1C_1\lambda\sinh(4\lambda\,\text{Ha}_1) + \\ + 8A_1S_1\cosh(2\lambda\,\text{Ha}_1) + 8C_1S_1\sinh(2\lambda\,\text{Ha}_1) + 8\lambda\,\text{Ha}_1{}^2\,S_1{}^2] \tag{56}$$

$$N_2 = -\frac{\text{Ec}_1\,\text{Pr}_1}{4\lambda}[\lambda(A_1^2 + C_1^2)\cosh(2\lambda\,\text{Ha}_1) + 2A_1C_1\lambda\sinh(2\lambda\,\text{Ha}_1) + \\ + 8A_1S_1\cosh(\lambda\,\text{Ha}_1) + 8C_1S_1\sinh(\lambda\,\text{Ha}_1) + 2\lambda\,\text{Ha}_1{}^2\,S_1{}^2] \tag{57}$$

$$N_3 = -\frac{\text{Ec}_2\,\text{Pr}_2}{4\lambda}[\lambda(A_2^2 + C_2^2)\cosh(2\lambda\,\text{Ha}_2) + 2A_2C_2\lambda\sinh(2\lambda\,\text{Ha}_2) + \\ + 8A_2S_2\cosh(\lambda\,\text{Ha}_2) + 8C_2S_2\sinh(\lambda\,\text{Ha}_2) + 2\lambda\,\text{Ha}_2{}^2\,S_2{}^2] \tag{58}$$

$$N_4 = -\frac{\text{Ec}_2\,\text{Pr}_2}{4\lambda}[\lambda(A_2^2 + C_2^2) + 8A_2S_2] \tag{59}$$

$$N_5 = -\frac{\mathrm{Ec}_3\,\mathrm{Pr}_3}{4\lambda}[\lambda(A_3^2 + C_3^2) + 8A_3S_3] \tag{60}$$

$$N_6 = -\frac{\mathrm{Ec}_3\,\mathrm{Pr}_3}{4\lambda}[\lambda(A_3^2 + C_3^2)\cosh(2\lambda\,\mathrm{Ha}_3) - 2A_3C_3\lambda\sinh(2\lambda\,\mathrm{Ha}_3) +$$
$$+ 8A_3S_3\cosh(\lambda\,\mathrm{Ha}_3) - 8C_3S_3\sinh(\lambda\,\mathrm{Ha}_3) + 2\lambda\,\mathrm{Ha}_3{}^2\,S_3{}^2] \tag{61}$$

$$N_7 = -\frac{\mathrm{Ec}_1\,\mathrm{Pr}_1}{4\lambda}[2\lambda^2\,\mathrm{Ha}_1(A_1^2 + C_1^2)\sinh(2\lambda\,\mathrm{Ha}_1) + 4\lambda^2\,\mathrm{Ha}_1\,A_1C_1\cosh(2\lambda\,\mathrm{Ha}_1) +$$
$$+ 8\lambda\,\mathrm{Ha}_1\,A_1S_1\sinh(\lambda\,\mathrm{Ha}_1) + 8\lambda\,\mathrm{Ha}_1\,C_1S_1\cosh(\lambda\,\mathrm{Ha}_1) + 4\lambda\,\mathrm{Ha}_1{}^2\,S_1{}^2] \tag{62}$$

$$N_8 = -\xi_1\frac{\mathrm{Ec}_2\,\mathrm{Pr}_2}{4\lambda}[2\lambda^2\,\mathrm{Ha}_2(A_2^2 + C_2^2)\sinh(2\lambda\,\mathrm{Ha}_2) + 4\lambda^2\,\mathrm{Ha}_2\,A_2C_2\cosh(2\lambda\,\mathrm{Ha}_2) +$$
$$+ 8\lambda\,\mathrm{Ha}_2\,A_2S_2\sinh(\lambda\,\mathrm{Ha}_2) + 8\lambda\,\mathrm{Ha}_2\,C_2S_2\cosh(\lambda\,\mathrm{Ha}_2) + 4\lambda\,\mathrm{Ha}_2{}^2\,S_2{}^2] \tag{63}$$

$$N_9 = -\frac{\mathrm{Ec}_2\,\mathrm{Pr}_2}{4\lambda}(4\lambda^2\,\mathrm{Ha}_2\,A_2C_2 + 8\lambda\,\mathrm{Ha}_2\,C_2S_2) \tag{64}$$

$$N_{10} = -\xi_2\frac{\mathrm{Ec}_3\,\mathrm{Pr}_3}{4\lambda}(4\lambda^2\,\mathrm{Ha}_3\,A_3C_3 + 8\lambda\,\mathrm{Ha}_3\,C_3S_3) \tag{65}$$

Results and discussion

In this section, flow and heat transfer results for MHD flow of three immiscible fluids in a horizontal channel with isothermal walls in the presence of an applied electric and inclined magnetic are presented and discussed for various values of selected parameters. Dimensionless velocity, temperature and magnetic field induction are presented graphically in figs. 2-22 for the three fluids important for technical practice in order to elucidate the significant features of the hydrodynamic and thermal state of the flow. Figures 2-4 depict the effect of the Hartmann number on velocity, temperature and induced magnetic field, while the electrical loading parameter, K, is equal to zero (so-called short-circuit condition). Figure 2 shows the velocity profiles over the channel height for several values of the Hartmann number. It can clearly be seen that as the Hartmann number is increased the velocity profiles become flatter because application of a transverse magnetic field normal to the flow direction has a tendency to create a drag-like Lorentz force which has a decreasing effect on the flow velocity. The influence of the Hartmann number on the velocity field was most pronounced in the channel region III containing the fluid with greatest electrical conductivity.

Effect of increasing the Hartman number on the ratio of induced and applied magnetic field is shown in fig. 3. This ratio decreases with increase of the Hartmann number. Ratio of an induced and applied magnetic field is more pronounced in the channel region II and III containing more conductive fluids. The influence of the induced magnetic field for chosen fluids in the considered case is not so pronounced, but in case of higher values of the magnetic Reynolds number, the knowledge of the applied and induced field ratio have great significance. It is characteristic that the induced magnetic field leads to the occurrence of transverse pressure gradient, without changing the hydrodynamics of flow. Increase of the transverse pressure gradient may lead to flow instability at the interface of the fluids. Figure 4 shows the influence of the Hartmann number on the dimensionless temperature. Several interesting ob-

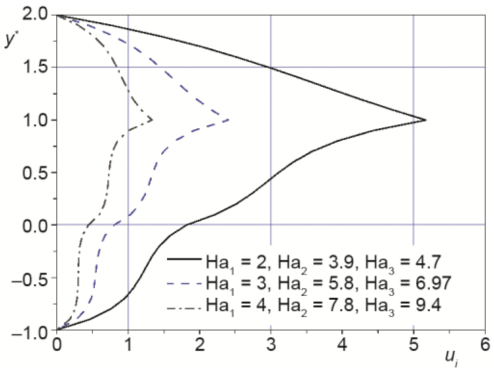

Figure 2. Velocity profiles for different values of Hartmann numbers

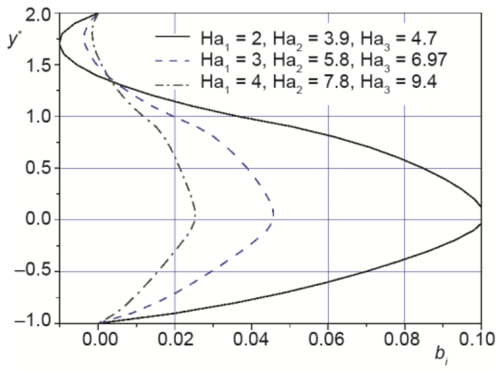

Figure 3. Ratio of an induced and applied magnetic field for different values of Hartmann numbers

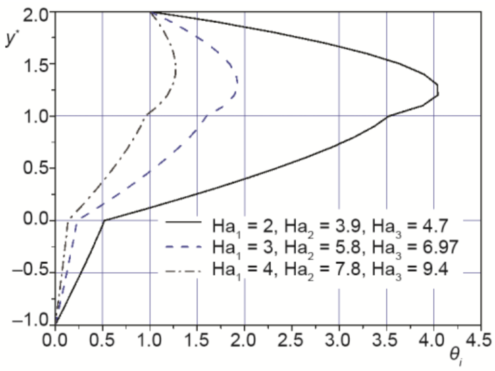

Figure 4. Temperature profiles for different values of Hartmann numbers

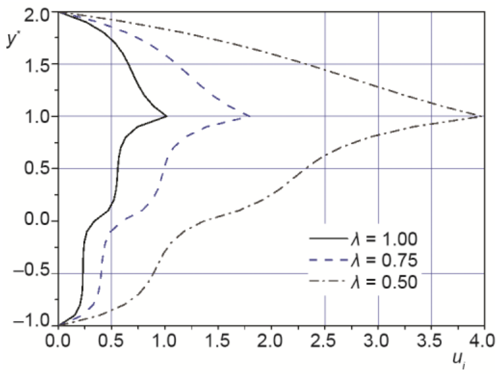

Figure 5. Velocity profiles for different magnetic field inclination angle

servations can readily be made. First, it should be recalled that, in the solution, both viscous heating and Joule heating were included in the analysis. Viscous heating is more pronounced in area near upper plate, and at the interface of regions I and II, while Joule heating and conduction dominates in the regions II and III. In general, the effect of Hartman number increasing on temperature profiles in all three fluid regions is reflected in equalizing the fluid temperatures, as well as in the reduction of temperatures, which is in accordance with the conclusions given by Shaaban and Abou-Zeid [28]. Figures 5-7 show the effect of the magnetic field inclination angle on the distribution of velocity, temperature and the ratio of the applied and induced magnetic field. Figure 5 shows the effect of the angle of inclination on velocity which predicts that the velocity increases as the inclination angle increases. These results are expected because increase of magnetic field inclination angle reduces the Lorentz force which has a decreasing effect on the flow velocity. In fig. 6, the dimensionless temperature distribution as a function of y^* for various values of applied magnetic field inclination angle, is shown. It can be seen from figs. 5 and 6 that the magnetic field flattens out the velocity and temperature profiles and reduces the flow energy transformation as the inclination angle decreases. The ratio of an induced and externally imposed magnetic field, for the short circuit condition and various values of magnetic field inclination, is shown in fig. 7.

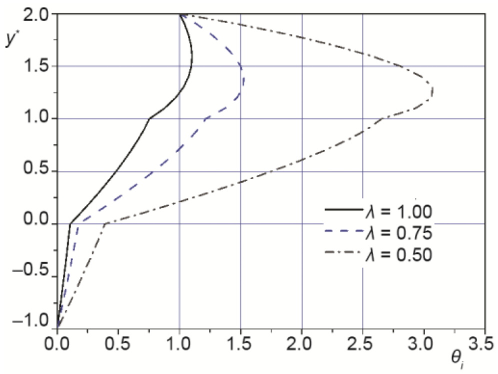

Figure 6. Temperature profiles for different magnetic field inclination angle

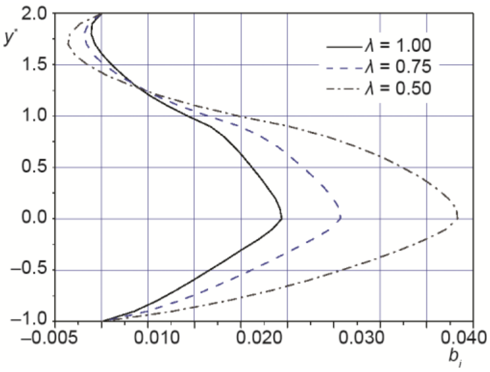

Figure 7. Ratio of an induced and applied magnetic field for different magnetic field inclination angle

Disturbance of the external magnetic field is directly proportional to the magnetic Reynolds number and essentially depends on the regime of the channel load and inclination of the applied magnetic field. In the observed case the magnetic Reynolds numbers are small and hence the induced field is small, but the general conclusions represented in the paper are valid also for higher values. Figure 7 shows increase in the ratio of magnetic fields as the inclination angle of an applied field decreases. In observed case the maximum value is observed at the interface of fluids in regions II and III.

The effect of the ratio of fluids viscosities in regions I, II, and III on the velocity, induced magnetic field and temperature is shown in figs. 8-13. In the case of parameter α_1 alteration, the change in velocity is significant in regions I and II, while in the case of parameter α_2 velocity remains almost constant. These results are given for the same magnetic field intensity, and it can be concluded that the dominant effect of changes in fluid viscosity occurs in region I, while this influence in other two regions is much less pronounced. The ratio of induced and externally imposed magnetic field for different values of fluids viscosities ratio is shown in figs. 10 and 11. Obtained results shows that change of fluid viscosities have very little influence on induced magnetic field. The effect of the fluids viscosities ratio on temperature field is shown in the figs. 12 and 13. Increase of parameter α_1 significantly increases the temperature field for fluids in regions I and II. The effect of parameter α_2 has opposite influence on temperature of fluids in regions I and II. In region III temperature remain almost constant for all values of the fluids viscosities ratios α_1 and α_2. In this region the dominant form of heat transfer is conduction. The effect of the ratio of electrical conductivities of the fluids on the velocity profiles is shown in figs. 14 and 15. It can clearly be seen that as the ratio of electrical conductivities γ_1 is increased, the velocity profile for the fluid in region I becomes flatter, while the fluid in region II obtain laminar profile. As the electrical conductivity of the lower fluid does not change, change of velocity in region II is expressed at the interfaces and this is a consequence of the mutual effects of fluids. As for certain fluids used in technical practice is very easy to change the electrical conductivity without significant changes in other physical properties, it is interesting to consider the influence of electrical conductivities ratio on the

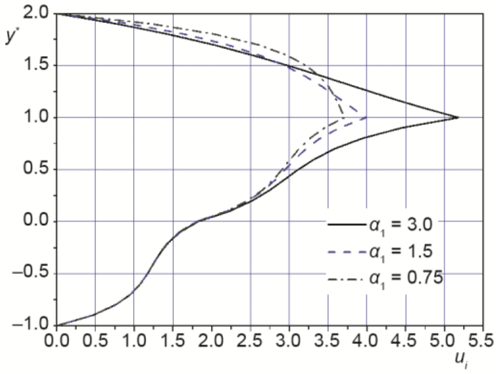

Figure 8. Velocity profiles for different ratios of fluids viscosities α_1

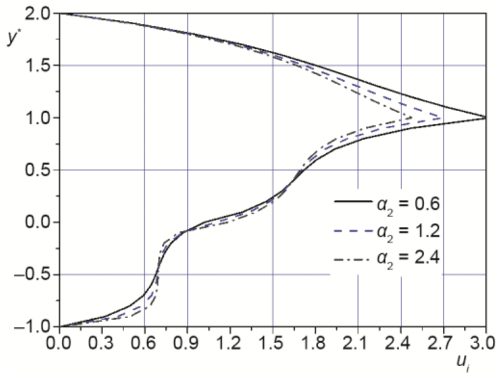

Figure 9. Velocity profiles for different ratios of fluids viscosities α_2

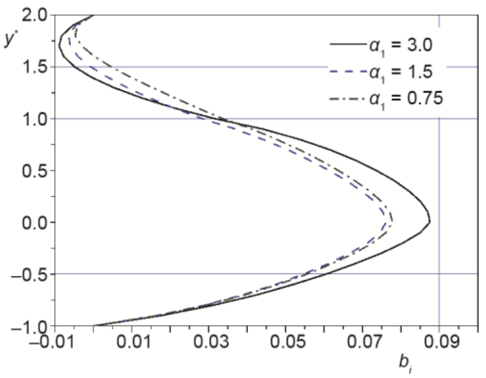

Figure 10. Ratio of an induced and applied magnetic field for different ratios of fluids viscosities α_1

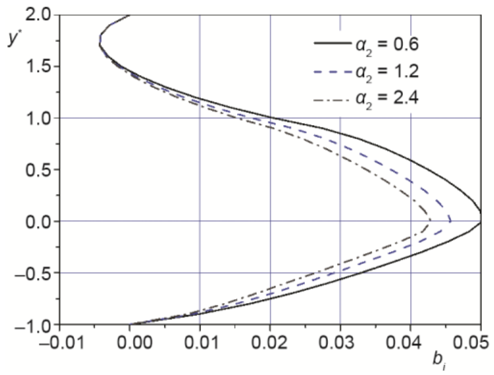

Figure 11. Ratio of an induced and applied magnetic field for different ratios of fluids viscosities α_2

temperature, velocity and induced magnetic field. In case of change of the ratio of electrical conductivities γ_2, the velocity profiles in all three regions changes significantly. Change of electrical conductivity of fluid in region III cause the velocity change in all three fluids regions, which is consequence of Lorentz force decreasing. Influence of fluids physical properties at the interface shows much more pronounced effects in this case.

In figs. 16 and 17 the temperature distribution as a function of y^*, for various values of the ratio of electrical conductivities is shown. The effect of ratio of fluids electrical conductivities on temperature field is pronounced only in regions I and II. Temperature field in region III remain constant for all values γ_1 and γ_2. It is found that the effect of increasing γ is to decrease the temperature field in the regions I and II. In the case of decreasing of ratio of electrical conductivities viscous dissipation for fluids in regions I and II was expressed, while the Joule heating is increased in the case of increase of parameters γ_1 and γ_2. Although the increase of conductivities ratio γ_1 significantly reduces the velocity in region I, the total temperature increases due to Joule heating and mutual effects of fluids at the interface. The effect of the ratio of electrical conductivities of the fluids on the induced magnetic field is shown in figs. 18 and 19. It is interesting to note that the increase of both parameters γ_1 and γ_2 changes significantly the ratio of induced and applied magnetic field in all three regions. For certain values of parameters when the electrical conductivities of the fluids have similar values profiles of induced field becomes very similar to Hartmann flow. The difference in relation to the Hartmann flow is reflected in the incomplete symmetry around the axis of the channel. A significant increase of the parameters γ_1 and γ_2 changes the direction of induced field in all three fluid regions. Of particular significance is the analysis when the loading factor, *K*, is different from zero (value of loading factor, *K*, define the system as generator, flowmeter or pump), while the Hartmann number is constant. The introduction of parameter, *K*, modifies the usual Hartmann flow. In addition, for a given Hartmann number, the relationship between pressure gradient and mean flow or flow rate is altered by *K*. In the case when *K* = 0 the external electric field plays the role of a supplementary pressure gradient.

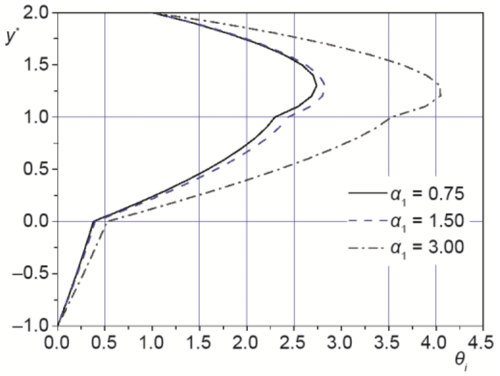

Figure 12. Temperature profiles for different ratios of fluids viscosities α_1

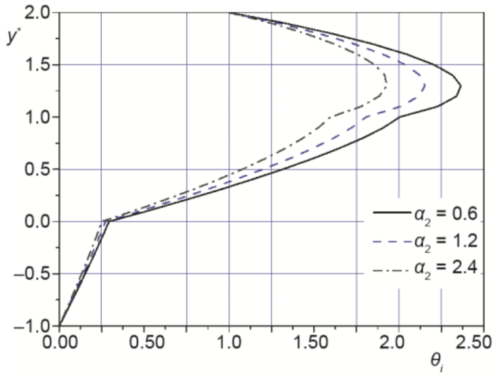

Figure 13. Temperature profiles for different ratios of fluids viscosities α_2

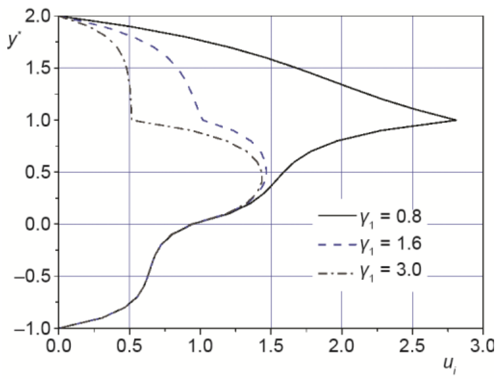

Figure 14. Velocity profiles for different values of electrical conductivities ratio γ_1

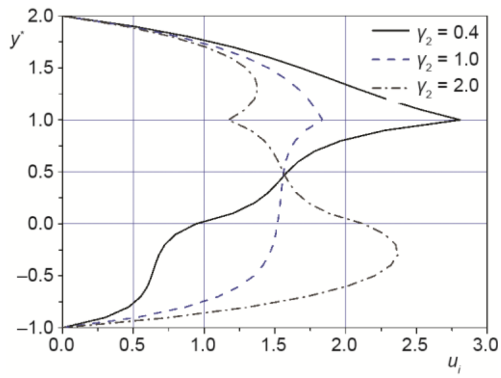

Figure 15. Velocity profiles for different values of electrical conductivities ratio γ_2

Figure 21 shows the effect of the loading factor on velocity, which predicts the possibility to change the flow direction. As can be seen, for a fixed Hartman number, a *K* = 2 will decrease the pressure gradient while a *K* = –2 will increase it. Also, significant increase in the flow is achieved for negative values of *K*. The obtained results show that different values of the inclination angle, the Hartmann number and the load factor is a convenient control method for heat and mass transfer processes. In fig. 20 the temperature distribution as a function of y^*, for various values of *K*, is shown.

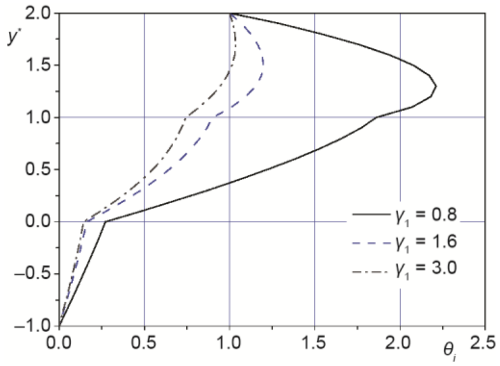

Figure 16. Temperature profiles for different values of electrical conductivities ratio γ_1

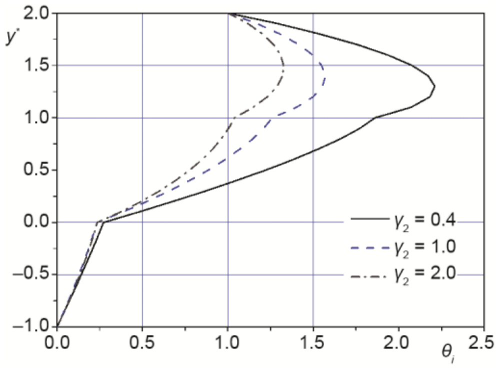

Figure 17. Temperature profiles for different values of electrical conductivities ratio γ_2

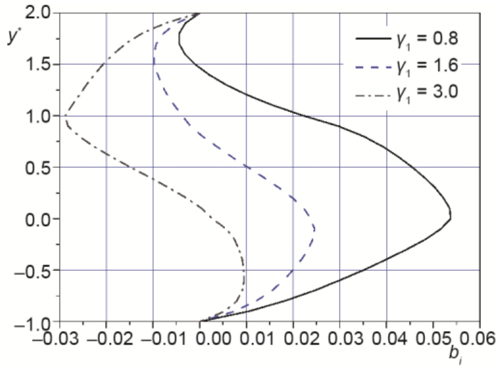

Figure 18. Ratio of an induced and applied magnetic field for different values of electrical conductivities ratio γ_1

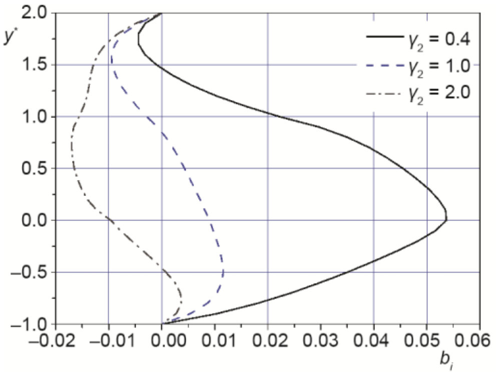

Figure 19. Ratio of an induced and applied magnetic field for different values of electrical conductivities ratio γ_2

When $K = 0$ the channel is short-circuited and all current flows in one direction. In this case the temperature distribution is affected by the viscous dissipation and Joule heating. Temperature rise is particularly pronounced in the region I, while in other two regions the temperature remains almost constant. On account of this increase, the temperature of fluid in region II slightly increases at the interface. The ratio of an induced and externally imposed magnetic field had a considerable change when the loading parameter, K, was different from zero, (fig. 22). When $K = –2$, all the current flows to the right in the channel, and it must be presumed that this net current flow has been supplied by an external power supply. Similar curves apply for $K = 2$, except that the magnetic induction lies in the other direction, as a result of current flowing in the opposite direction.

Conclusion

The problem of MHD flow and heat transfer of three immiscible fluids between parallel plates in the presence of applied magnetic field was investigated analytically. All three fluids were assumed Newtonian and electrically conducting. Closed form solutions for dimensionless velocity and temperature of each fluid were obtained taking into consideration suitable interface matching conditions and boundary conditions. The results were numerically

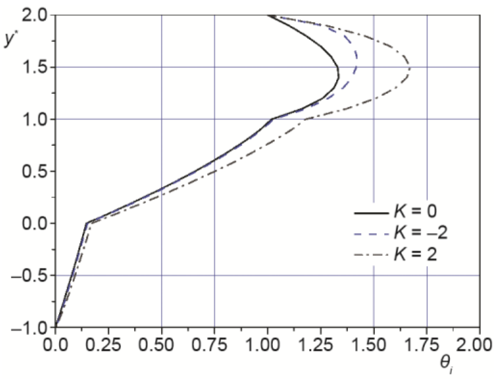

Figure 20. Temperature profiles for different values of load factor

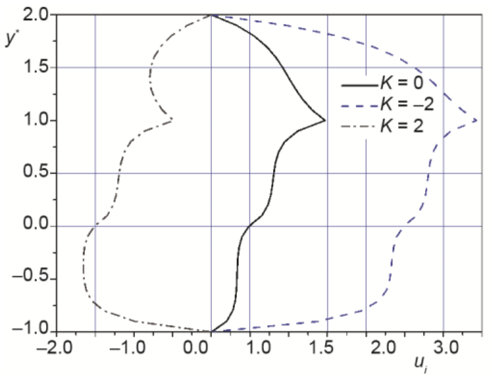

Figure 21. Velocity profiles for different values of load factor

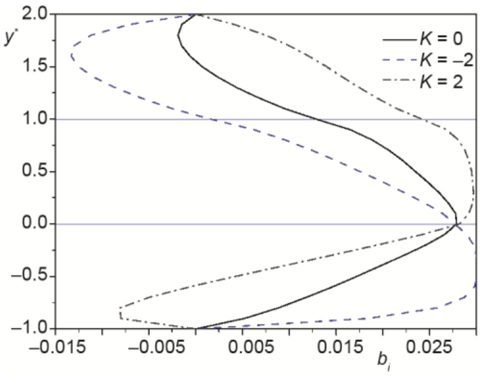

Figure 22. Ratio of an induced and applied magnetic field for different values of load factor

evaluated and presented graphically for three fluids. Only the part of the results is presented for various values of Hartmann number and ratios of viscosities and thermal conductivities. The obtained results show that the control of flow and heat transfer for observed case can be realized by changing the magnetic field intensity and defined ratios of fluid properties.

Acknowledgment

This paper is supported by the Serbian Ministry of Sciences and Technological development. Project No. TR 35016-Research of MHD flow in the channels, around the bodies and application in the development of the MHD pump.

References

[1] Blum, E. Ya., Heat and Mass Transfer in MHD Flow Past Bodies, *Magnetohydrodynamics, 6* (1970), 2, pp. 212-218
[2] Cramer, K. R., Pai, S. I., *Magnetofluid Dynamics for Engineers and Applied Physicists*, McGraw-Hill, New York, USA, 1973
[3] El-Dabe, N., *et al.*, Magnetohydrodynamic Non-Newtonian Nanofluid Flow over a Stretching Sheet through a Non-Darcy Porous Medium with Radiation and Chemical Reaction, *Journal of Computational and Theoretical Nanoscience*, *12* (2015), 12, pp. 5363-5371
[4] Attia, H. A., Hall Current Effects on the Velocity and Temperature Fields of an Unsteady Hartmann Flow, *Canadian Journal of Physics*, *76* (1998), 9, pp. 739-746
[5] Kiyasatfar, M., *et al.*, Investigation of Thermal Behavior and Fluid Motion in DC Magnetohydrodynamic Pumps, *Thermal Science*, *18* (2014), Suppl. 2, pp. S551-S562
[6] Chandrasekhar, S., Sharma, V. M., Brownian Heat Transfer Enhancement in the Turbulent Regime, *Facta Universitatis Series: Mechanical Engineering*, *14* (2016), 2, pp. 169-177
[7] Abou-Zeid, M., Homotopy Perturbation Method for MHD Non-Newtonian Nanofluid Flow through a Porous Medium in Eccentric Annuli with Peristalsis, *Thermal Science*, *21* (2017), 5, pp. 2069-2080
[8] Ghosh, S. K., Nandi, D. K., Magnetohydrodynamic Fully Developed Combined Convection Flow between Vertical Plates Heated Asymmetrically, *Journal of Technical Physics*, *41* (2000), 2, pp. 173-185

[9] Bodosa, G., Borkakati, K., MHD Couette Flow with Heat Transfer between Two Horizontal Plates in the Presence of a Uniform Transverse Magnetic Field, *Journal of Theoretical and Applied Mechanics*, *30* (2003), 1, pp. 1-9
[10] Ghosh, S. K., *et al.*, Hydromagnetic Free Convection Flow with Induced Magnetic Field Effects, *Meccanica*, *45* (2010), 2, pp. 175-185
[11] Borkakati, A. K., Chakrabarty, S., Unsteady Free Convection MHD Flow between Two Heated Vertical Parallel Plates in Induced Magnetic Field, *Indian Journal of Theoretical Physics*, *47* (1999), 1, pp. 143-160
[12] Aydin, O., Avci, M., Laminar Forced Convection with Viscous Dissipation in a Couette-Poiseuille Flow between Parallel Plates, *Applied Energy*, *83* (2006), 8, pp. 856-867
[13] Singha, K. G., Analytical Solution to the Problem of MHD Free Convective Flow of an Electrically Conducting Fluid between Two Heated Parallel Plates in the Presence of an Induced Magnetic Field, *International Journal of Applied Mathematics and Computation*, *1*, (2009), 4, pp. 183-193
[14] Shail, R., On Laminar Two-Phase Flows in Magnetohydrodynamics, *International Journal of Engineering Science*, *11* (1973), 10, pp. 1103-1108
[15] Lohrasbi, J., Sahai, V., Magnetohydrodynamic Heat Transfer in Two-Phase Flow between Parallel Plates, *Applied Scientific Research*, *45* (1988), 1, pp. 53-66
[16] Malashetty, M. S., *et al.*, Two Fluid Flow and Heat Transfer in an Inclined Channel Containing Porous and Fluid Layer, *Heat and Mass Transfer*, *40* (2004), 11, pp. 871-876
[17] Abou-Zeid, M., Magnetohydrodynamic Boundary Layer Heat Transfer to a Stretching Sheet Including Viscous Dissipation and Internal Heat Generation in a Porous Medium, *Journal of Porous Media*, *14* (2011), 11, pp. 1007-1018
[18] Umavathi, J. C., *et al.*, Unsteady Two-Fluid Flow and Heat Transfer in a Horizontal Channel, *Heat and Mass Transfer*, *42* (2005), 2, pp. 81-90
[19] Nikodijević, D., *et al.*, Flow and Heat Transfer of Two Immiscible Fluids in the Presence of Uniform Inclined Magnetic Field, Hindawi Publishing Corporation, *Mahtematical Problems in Engineering*, *2011* (2011), ID 132302
[20] Haiwang, L., *et al.*, Analytical Model of Mixed Electroosmotic/Pressure Driven Three Immiscible Fluids in a Rectangular Microchannel, *International Journal of Heat and Mass Transfer*, *52* (2009), 19-20, pp. 4459-4469
[21] Hormozia, S., *et al.*, Multi-Layer Channel Flows with Yield Stress Fluids, *Journal of Non-Newtonian Fluid Mechanics*, *166* (2011), 5-6, pp. 262-278
[22] Li, J., *et al.*, Analysis of Multi-Layer Immiscible Fluid Flow in a Microchannel, *Journal of Fluids Engineering*, *133* (2011), 11, pp. 1-10
[23] Haim, H. B., *et al.*, A Magneto-Hydrodynamically Controlled Fluidic Network, *Sensors and Actuators B*, *88* (2003), 2, pp. 205-216
[24] Hussameddine, S. K., *et al.*, Analytical Prediction of Flow Field in Magnetohydrodynamic-Based Microfluidic Devices, *Journal of Fluids Engineering*, *130* (2008), 9, ID 091204
[25] Yi, M., *et al.*, A Magnetohydrodynamic Chaotic Stirrer, *Journal of Fluid Mechanics*, *468* (2002), Oct., pp. 153-177
[26] Weston, M. C., *et al.*, Magnetic Fields for Fluid Motion, *Analytical Chemistry*, *82* (2010), 9, pp. 3411-3418
[27] Thorn, R., *et al.*, Three-Phase Flow Measurement in the Petroleum Industry, *Measurement Science and Technology*, *24* (2013), 1, pp. 1‑17
[28] Shaaban, A., Abou-Zeid, M., Effects of Heat and Mass Transfer on MHD Peristaltic Flow of a Non-Newtonian Fluid through a Porous Medium between Two Coaxial Cylinders, *Mathematical Problems in Engineering*, *2013* (2013), ID 819683

Paper submitted: May 21, 2018
Paper revised: October 11, 2018
Paper accepted: October 12, 2018